3D Printed Palladium Catalyst for Suzuki-Miyaura Cross-coupling Reactions

Evgeny Bulatov,[a, b] Elmeri Lahtinen,[a] Lauri Kivijärvi,[a] Evamarie Hey-Hawkins,*[c] and Matti Haukka*[a]

Selective laser sintering (SLS) 3d printing was utilized to manufacture a solid catalyst for Suzuki-Miyaura cross-coupling reactions from polypropylene as a base material and palladium nanoparticles on silica (SilicaCat Pd^0 R815-100 by SiliCycle) as the catalytically active additive. The 3d printed catalyst showed similar activity to that of the pristine powdery commercial catalyst, but with improved practical recoverability and reduced leaching of palladium into solution. Recycling of the printed catalyst led to increase of the induction period of the reactions, attributed to the pseudo-homogeneous catalysis. The reaction is initiated by oxidative addition of aryl iodide to palladium nanoparticles, resulting in formation of soluble molecular species, which then act as the homogeneous catalyst. SLS 3d printing improves handling, overall practicality and recyclability of the catalyst without altering the chemical behaviour of the active component.

1. Introduction

The technology of additive manufacturing, broadly known as three-dimensional (3d) printing, has been evolving extensively in the last decades, and recently catalytically active 3d printed objects started to emerge.[1–13] Indeed, 3d printing provides potential for creating objects not only with desired catalytic properties, but at the same time with required shapes, e.g. for batch or flow reactors with heterogeneous solid catalysts. A number of reports emerged recently on new catalysts for various reactions, produced by 3d printing with[1–6] and without[7–13] chemical post-processing of the printed objects. Among these reports, the majority utilizes fused deposition modelling (FDM) or robocasting,[1–4,7–12] selective laser melting (SLM),[5,6] and in some cases stereolithography (SL)[13] methods. However, these reported methods possess several drawbacks. Thus, all these methods put significant restrictions on the materials used for 3d printing and often require their pre-processing. In addition, such methods produce monolithic objects with no inherent porosity, and a significant part of catalytically active material inside the bulk of a 3d printed object remains inaccessible for the reactants. Catalysts can be deposited on the surface of 3d printed objects by means of chemical post-processing, but such an approach significantly lessens the advantages of 3d printing by expanding the manufacturing procedure.

Selective laser sintering (SLS) 3d printing is a suitable method for manufacturing objects with inherent flow-through porosity, and catalytically active additives can be added without pre- or post-processing.[14–18] In an SLS process, a powder is sintered by a moving infrared laser, forming 3d objects in a layer-by-layer fashion. Catalytically active additives in powder form can be simply mixed with the base powder, and the porosity of the printed objects can be controlled by changing the particle size of the powder and adjusting the printing parameters, such as temperature, and power and speed of the laser. Therefore, SLS 3d printing allows fabrication of solid but highly porous objects, in which fluid can flow through the voids between the partially fused particles, making catalysts within the bulk of the object accessible for contact with the reaction medium. We have previously demonstrated the applicability of SLS 3d printing for the production of porous filters with various absorption properties,[14,15] flexible carbonous electrodes,[16] and heterogeneous hydrogenation catalysts,[17,18] and in this work we further develop catalytically active 3d printed materials with implementation in Suzuki-Miyaura cross-coupling reaction.

Reported for the first time in 1979,[19] the Suzuki-Miyaura cross-coupling reaction, in which a palladium catalyst mediates the reaction between vinyl or aryl halides and organoboronic acids or esters in the presence of a base, has found broad application in synthetic chemistry and eventually has been acknowledged with the Nobel Prize in 2010.[20] However, the homogeneously catalyzed reaction possesses the drawbacks of

[a] E. Bulatov, E. Lahtinen, L. Kivijärvi, Prof. M. Haukka
Department of Chemistry
University of Jyväskylä
P.O. Box 35
40014 Jyväskylä (Finland)
E-mail: matti.o.haukka@jyu.fi
[b] E. Bulatov
Department of Chemistry
University of Helsinki
A.I. Virtasen aukio 1, P.O. Box 55
00014 Helsinki (Finland)
[c] Prof. E. Hey-Hawkins
Faculty of Chemistry and Mineralogy
Institute of Inorganic Chemistry
Leipzig University
Johannisallee 29
04103 Leipzig (Germany)
E-mail: hey@uni-leipzig.de

Supporting information for this article is available on the WWW under https://doi.org/10.1002/cctc.202000806

problematic recovery of the catalyst and contamination of the product by the catalyst, which create additional obstacles particularly in the production of pharmaceuticals.[21] Accordingly, the possibility of heterogeneous catalysts has been widely studied, with the two main approaches being immobilization (anchoring) of the complexes on a support and application of supported metallic palladium,[22] even though dynamic nature of catalysis on the surface and/or solution is often behind the apparent heterogeneous behaviour of such catalysts.[23] Palladium nanoparticles (NPs) are known to be particularly active in catalytic reactions and have several advantages for SLS 3d printing, such as easier preparation and higher stability under 3d printing conditions (air and elevated temperatures), compared to anchored molecular catalysts.[24,25] Therefore, in this study SLS 3d printing was used to produce objects with catalytic activity in Suzuki-Miyaura cross-coupling reactions from a commercially available catalyst based on palladium NPs supported on silica.

2. Results and Discussion

2.1. Preparation of the catalyst

Commercially available palladium NPs on silica (Pd/SiO_2, SilicaCat Pd^0 R815-100 by SiliCycle) were used as the catalytically active additive for the 3d printed objects. High catalytic activity of this material has been documented in literature,[26] whereas its heterogeneous mode of catalysis has been questioned, and more recent studies suggest dominating pseudo-homogeneous mode of catalysis by leached palladium,[27] which is commonly observed for various supported palladium NP catalysts.[24,28,29]

In order to demonstrate the potential of the SLS 3d printing technology to create functional objects of various shapes, 3d printed sleeves for magnetic stirring bars were fabricated (Figure 1). Impregnation of Teflon coated magnetic stirrers with transition metals has been suggested as an attractive approach to fabrication of reusable catalysts,[30–32] and our group has advanced this idea by implementing removable 3d printed sleeves for stirring bars.[17,18] Such design provides the advantages of constant renewal of the liquid layer around the catalyst during the reaction due to stirring, and easy removal of the catalyst from the reaction mixture by using a magnetic rod. Flexibility of polypropylene, used as the base material for 3d printing, allowed a tight fit of the sleeves on stirring bars without cracking.

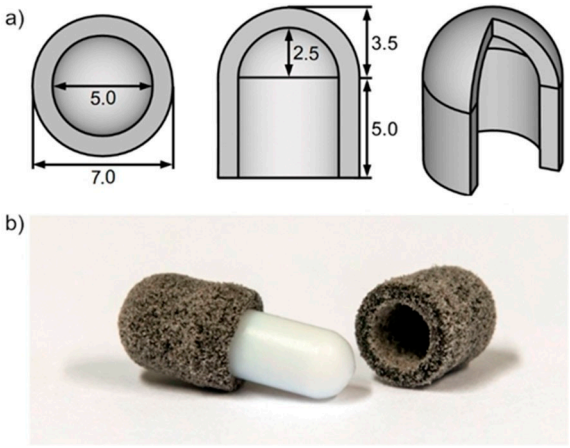

Figure 1. (a) Design (top, side, and perspective views; the dimensions are presented in mm) of the 3d printed catalyst sleeves for magnetic stirring bars; (b) Photograph of the printed objects.

2.2. Comparison between the 3d printed and original powder catalyst

The catalytic activity of the obtained 3d printed stirring bar sleeves was tested in a model Suzuki-Miyaura cross-coupling reaction (Scheme 1) and compared to that of equivalent (in relation to palladium load) amount of the pristine Pd/SiO_2 powder. The reaction conditions from the original publication on the SilicaCat catalyst were used,[26] except oxygen- and moisture-free atmosphere (in the original work the reactions were conducted under air) to avoid inconsistencies due to atmospheric variations and possible degradation of reaction intermediates in solution. The catalytic load was 0.2–0.5 mol% of palladium. Excess of phenylboronic acid pinacol ester (20%) allowed to suppress possible homocoupling reaction of aryl iodide, which could result in oxidation and deactivation of the catalyst. Potassium carbonate was used as the base in 50% excess, which allowed to negate the possible acid/base contribution from the polypropylene material used for 3d printing.

The produced 3d printed objects demonstrated good catalytic activity and recoverability in the test reaction with phenyl iodide, providing high yields of biphenyl in three consecutive cycles (Table 1). Leached palladium was detected in reaction solutions at about a hundred μg/l concentrations,

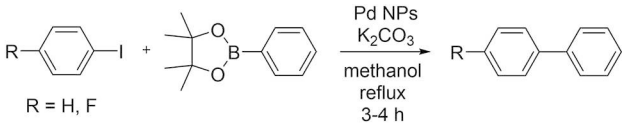

Scheme 1. The model Suzuki-Miyaura cross-coupling reaction used to test the catalytic activity of the 3d printed sleeves for magnetic stirring bars.

Table 1. Reaction yields and leached palladium in the repeated Suzuki-Miyaura cross-coupling reactions.[a]

Reaction cycle #	Yield of biphenyl [%][b]/[Pd] in solution [mg/l][c] 3d printed catalyst	Powder catalyst
1	99.5 / 0.11	92.0 / 0.81
2	83.3 / 0.09	78.2 / 0.42
3	87.5 / 0.18	83.4 / 0.28

[a] Performed in methanol under reflux with phenyl iodide and 0.2 mol% palladium load, reaction time 3 h. [b] Determined using GCMS. [c] Determined using ICP-OES.

which corresponds to about 1–2% of total palladium content in the catalyst leaching with each reaction cycle. In comparison, the equivalent amount of the pristine SilicaCat powder demonstrated slightly lower yields and significantly higher palladium leaching. The increased palladium content in solution was attributed to larger surface area of the powder.

Recycling of the powder catalyst appeared very difficult in practice, due to the required time and effort for filtration with unavoidable losses. On the other hand, the 3d printed catalyst could be recovered from the solution simply by using a magnetic rod (Figures S1,2 in supporting information), demonstrating that the implementation of SLS 3d printing allows great improvement of practical reusability of the catalyst, while not only maintaining its activity, but also reducing palladium depletion due to decreased leaching and eliminated losses caused by filtration.

2.3. Reusability of the 3d printed catalyst

In order to investigate the durability and reusability of the obtained objects, 10 repetitions of the test reactions were performed with the recycled catalyst. Since the change of reaction kinetics is a much more probative criterion of catalysts recoverability than reaction yields,[33] reaction progress and amount of leached palladium over time were followed in each cycle. To differentiate the products of possible homocoupling reactions, 4-fluorophenyl iodide was used in these experiments.

The extended repeated use of the catalyst resulted in gradual decrease of the reaction yields from quantitative to 82% in the last cycles, accompanied with the appearance and gradual increase of the induction period, resulting in sigmoidal kinetic curves (Figure 2a). The detected amounts of leached palladium in solution were increasing over time within one reaction (except for the first reaction), and generally decreasing with consecutive cycles (Figure 2b). No homocoupled products were observed.

Since reusability is among the key properties of the 3d printed catalyst, determination of the reason behind the appearance and gradual increase of the induction period at the start of the reactions can be vital for improving performance of the catalyst. In order to study the possible changes in physical structure of the catalytic objects, SEM images of outer surfaces and internal structures of the catalyst before and after the reactions were obtained. Analysis of the images revealed – typical for SLS 3d printed objects[14–18] – a highly porous structure both on the surface and in the bulk of the objects, which remained principally intact after 10 reaction cycles. The only observed changes were associated with the loss of loosely attached larger particles of sizes $\geq$100 μm, which did not undergo sintering during the 3d printing process due to their size (Figure 3). Having verified mechanical durability of the produced catalyst under the reaction conditions, we next turned to mechanistic studies of the reaction, since sigmoidal kinetics can indicate pseudo-homogeneous catalysis, taking place in solution after the true catalyst has leached from the solid phase pre-catalyst.[34]

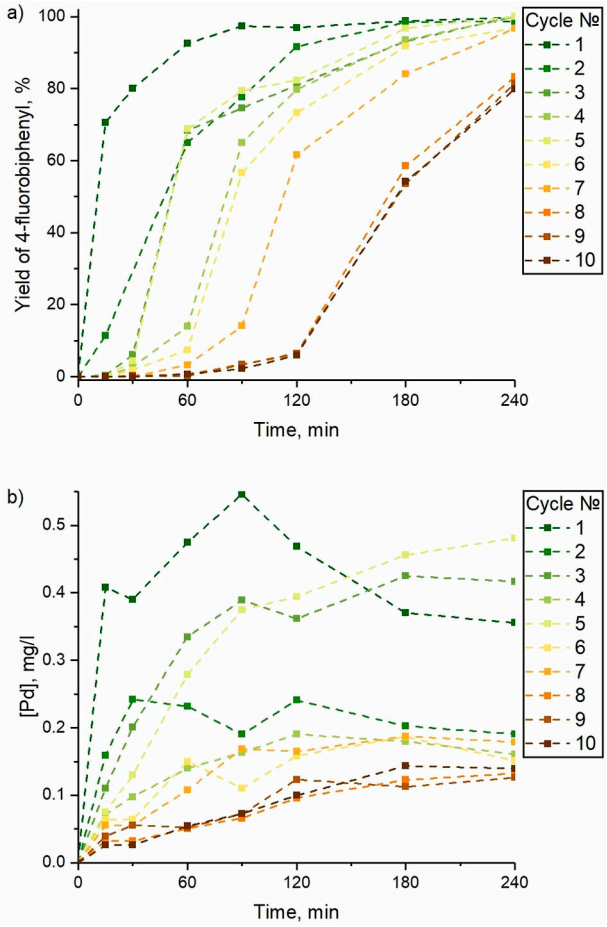

Figure 2. (a) Reaction progress and (b) concentration of leached palladium over time in 10 cycles of the test Suzuki-Miyaura cross-coupling reactions with the 3d printed catalyst (performed in methanol under reflux with 4-fluorophenyl iodide and 0.5 mol% palladium load, reaction time 4 h). Reaction yields and palladium concentrations were determined using GCMS and ICP-OES accordingly.

2.4. Mechanistic studies

Reliable determination of contributions of homogeneous and heterogeneous catalysis is a non-trivial task due to unavoidable leaching of palladium into solution, combined with its high catalytic activity,[24,28,29] and controversial results are present in literature regarding the mechanism of catalytic action of SilicaCat powder. Thus, heterogeneous nature of the catalyst in the reaction between 4-iodonitrobenzene and phenylboronic acid under ambient atmosphere has been demonstrated by the hot filtration test, in which the catalyst was filtered off before completion of the reaction, leading to an inert filtrate with no further conversion.[26] However, a single test like that may not be sufficient to make the conclusions on heterogeneous catalysis,[24,28] and the reported later flow split test indicated that the homogeneous contribution is dominant in the catalytic activity of SilicaCat powder in the reaction between 4-iodoacetophenone and phenylboronic acid under ambient atmosphere.[27] In light of the controversy in understanding of the mechanism of action of the catalyst, several tests were

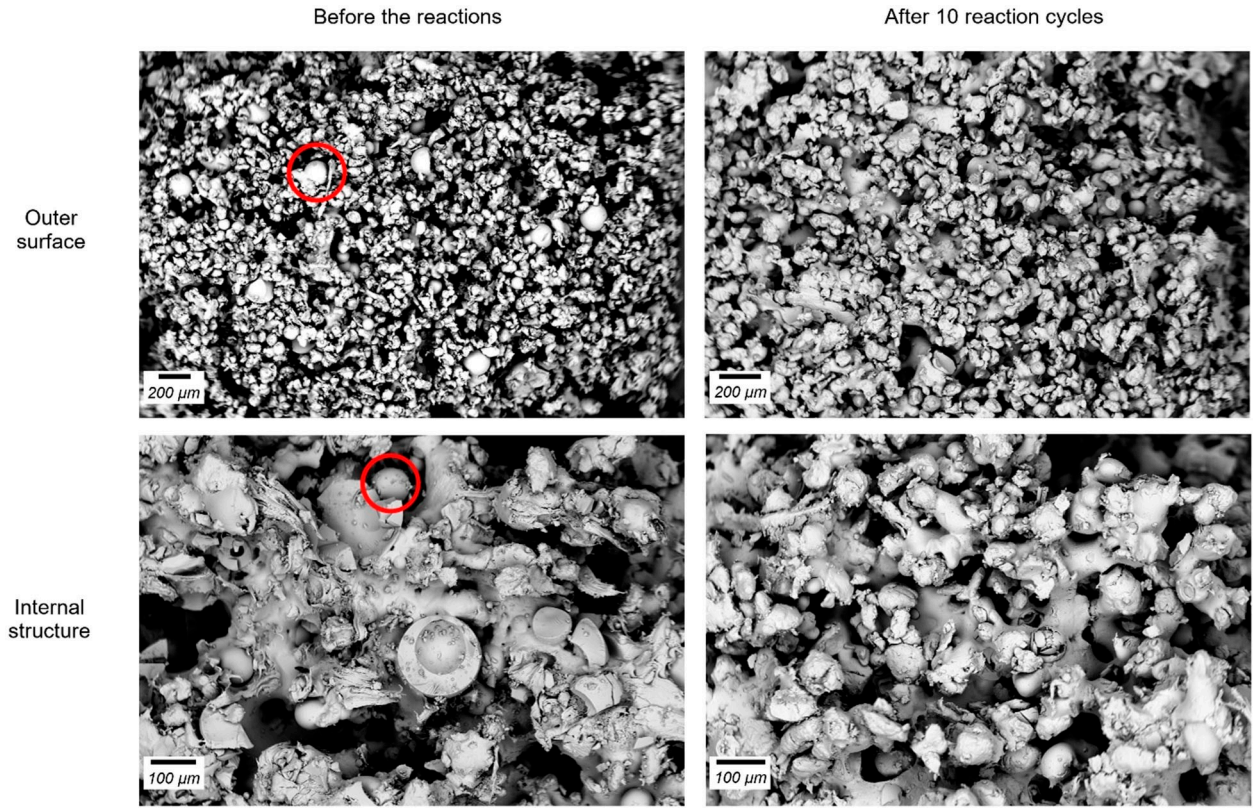

Figure 3. SEM images of outer surface (top) and internal structure (bottom) of the 3d printed catalytic objects before the reactions (left) and after 10 reaction cycles (right). Red circles highlight examples of unsintered polypropylene particles, which are lost after 10 reaction cycles.

performed in this work in order to elucidate whether the obtained 3d printed catalyst is truly heterogeneous or pseudo-homogeneous.

2.4.1. Catalytic activity tests

The mechanism of catalysis can be probed by studying catalytic performance under various reaction conditions, such as filtration of the catalyst in the course of the reaction, selective homo- and heterogeneous catalyst poisoning, and other.[28] The improved practicality of the 3d printed catalyst compared to the original powder allowed performing several tests in this work, including the filtration test, chelation test for homogeneous catalysts, and examination of catalytic activity of the filtrate after removal of the catalyst.

2.4.1.1. Filtration test

The reaction solution was filtered after 10 minutes of reflux and complete dissolution of the base, and the reaction was continued without the 3d printed catalyst. In contrast to the results reported for the original SilicaCat powder,[26] the removal of the catalyst before completion of the reaction did not prevent further reaction progress, but only slightly reduced the reaction rate in comparison with the reference reaction, indicating homogeneous catalysis (Figure 4, tests a and b).

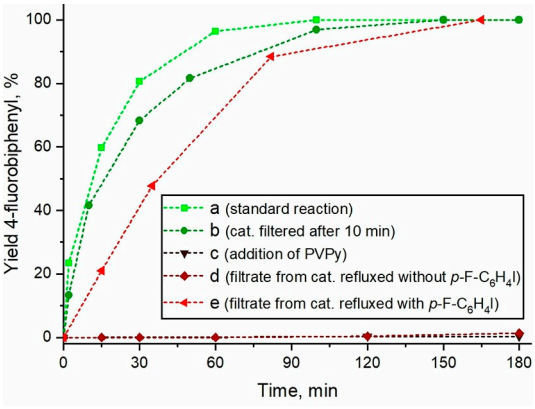

Figure 4. Reaction progress over time in the catalytic activity tests (a–e) with the 3d printed catalyst (performed in methanol under reflux with 4-fluorophenyl iodide and 0.5 mol% palladium load, reaction time 3 h). Reaction yields were determined using GCMS.

2.4.1.2. Chelation test

Addition of poly(4-vinylpyridine) (PVPy) can be used to test the heterogeneous activity of a solid phase palladium catalyst: this material is insoluble under the reaction conditions and possesses high affinity to form coordination compounds of palladium due to the abundant pyridine moieties. PVPy has been demonstrated previously to quench Heck coupling reactions catalyzed by a molecular palladium catalyst,[35] and was later used to verify the homogeneous catalysis by an anchored molecular catalyst[36] and dispersed nanoparticles.[37]

For the studied 3d printed catalyst, the presence of excess of PVPy (approximately 300 eq. relative to palladium) almost entirely prevented the reaction, providing the reaction yield of 0.3 % after 3 hours (Figure 4, test c).

However, the analysis of the palladium content in solution (Table 2 and discussion below in section 4.2) indicated that only a fraction of leached palladium was trapped by PVPy. It must be considered that palladium may leach in the form of coordination compounds (molecular leaching by dissociation of NPs) and soluble NPs (NP leaching by detachment from the support).[23,34,38] While PVPy effectively binds the molecular species, palladium NPs may remain in solution. Since the reaction is almost entirely quenched, it can be concluded that only the molecular palladium species are catalytically active under the reaction conditions, whereas supported and dissolved palladium NPs are not.

2.4.1.3. Homogeneous catalysis test

In this test, the 3d printed catalyst was refluxed under the reaction conditions with K_2CO_3 for 3 hours, filtered, and the yellowish filtrate was used as catalyst in the test reaction. Only trace catalytic activity was observed (reaction yield 1.3 % after 3 hours), despite the fact that significant quantities of leached palladium were detected in the filtrate (Figure 4, test d and Table 2, test f). However, when the catalyst was refluxed with the base and 4-fluorophenyl iodide, the filtrate possessed greenish colour and high reactivity, providing completion of the reaction in less than two hours (Figure 4, test e). Also, a significantly increased amount of leached palladium was detected in the filtrate in this case (Table 2, test h). Since the reaction between palladium NPs and aryl iodide (oxidative addition) is known to promote molecular palladium leaching,[34,38] this result supports the hypothesis that only the molecular palladium species possess homogeneous catalytic activity under the reaction conditions.

Table 2. Measured concentrations of palladium in solutions in the leaching tests (f–i) of the 3d printed catalyst.[a]

Test	[Pd], [mg/l][b]	Description
f	0.09	catalyst refluxed with the base
g	0.19	catalyst refluxed with the base and PVPy
h	0.68	catalyst refluxed with the base and 4-fluorophenyl iodide
i	0.35	catalyst refluxed with the base, 4-fluorophenyl iodide, and PVPy

[a] Performed in methanol under reflux with 0.5 mol% palladium load, reflux time 3 h. [b] Determined using ICP-OES.

2.4.2. Palladium leaching tests

In order to support the hypothesis that the leached palladium is present in solution partially in the form of catalytically inactive soluble NPs and partially as catalytically active molecular species, additional tests were performed to study the impact of PVPy and 4-fluorophenyl iodide on the leaching. In these tests, the 3d printed catalyst was refluxed in methanol under the reaction conditions with K_2CO_3 for 3 hours, with additions of PVPy and/or 4-fluorophenyl iodide.

2.4.2.1. Leaching with and without PVPy

The palladium contents in the filtrates from the catalyst refluxed with PVPy were slightly higher than without PVPy (Table 2, tests f and g), which appears surprising in the light of the capability of PVPy to trap dissolved palladium from solution.[35–37] On the other hand, the pyridine moieties in PVPy can act not only as trapping ligands for molecular palladium, but also as a base. As recently demonstrated by De Clercq and co-workers,[34] the additional base may facilitate palladium leaching in the form of soluble NPs. Moreover, there is a possibility of NP formation from the palladium trapped with PVPy, which can also leach into solution.[39] Since the addition of PVPy did quench the reaction (section 2.4.1.2 and Figure 4, test c), we speculate that all the molecular species were removed from the solution, whereas a shift of the sorption-desorption equilibrium and base-promoted NP leaching account for higher overall palladium content in solution after refluxing the catalyst with PVPy.

2.4.2.2. Leaching with and without PVPy in the presence of 4-fluorophenyl iodide

It has been well documented that molecular palladium species can form and leach into solution by the reaction of palladium NPs with aryl iodides.[34,38] Accordingly, the addition of an aryl iodide should increase the amount of the molecular species in solution, which can be captured by PVPy. In line with these considerations, the addition of PVPy reduced the palladium concentration by half when the catalyst was refluxed with 4-fluorophenyl iodide (Table 2, tests h and i). Notably, the addition of 4-fluorophenyl iodide resulted in increased overall palladium content in solution even in the presence of PVPy (Table 2, tests g and i), which can be explained by conversion of the leached molecular palladium into NP form.

The summary of the processes happening in the studied Suzuki-Miyaura cross-coupling reactions with 3d printed catalyst, deducted from the results described above, is depicted in Scheme 2. The reaction is initiated by the reaction between the solid palladium pre-catalyst and phenyl iodide or 4-fluorophen-

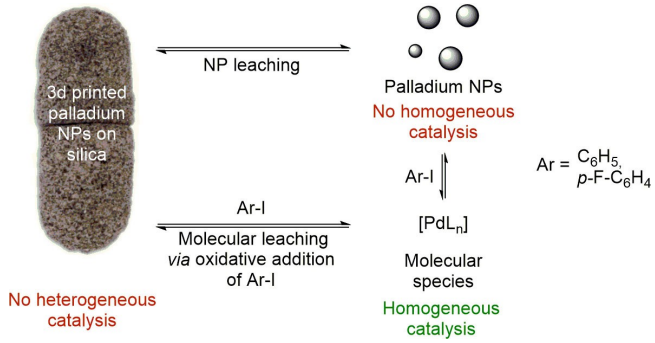

Scheme 2. Summary of the processes in the studied Suzuki-Miyaura cross-coupling reactions with the 3d printed catalyst.

yl iodide (oxidative addition), thus generating small amounts of catalytically active molecular species in solution, which then catalyze the homogeneous cross-coupling reaction. The active catalyst is only a fraction of all of the leached palladium, whereas the remaining palladium in solution is present in the form of leached palladium NPs, but does not contribute significantly to the catalytic activity. Supported nanoparticles do not contribute to cross-coupling catalysis either. In addition, it is likely that the NPs and molecular palladium species are in dynamic equilibrium, and there is a possibility that the two forms can be reabsorbed onto the solid support.[28] Therefore, the measurement of total palladium content in solution does not reflect the amount of active homogeneous catalyst. These factors may account for the absence of a clear reaction rate – palladium content correlation (Figure 2), which has been observed for some pseudo-homogeneous reactions.[34,40,41] Generally, such complex and dynamic systems have been observed and became an acknowledged feature of catalysis by metal NPs in the last decade.[23,42,43]

Therefore, the obtained catalyst operates in pseudo-homogeneous mode, in which after the initial heterogeneous oxidative addition step, the active catalyst is transferred into solution, enabling homogeneous catalysis. Such behaviour appears to be the intrinsic property of the catalytic additive in agreement with the recent study by de Bellefon and co-workers,[27] rather than an implication of SLS 3d printing used to manufacture the catalyst. The described catalytic mechanism explains the appearance and gradual increase of the induction period in the repeated reaction cycles (Figure 2a). Indeed, since easily accessible for oxidative addition palladium dissolves in the solution with every reaction cycle, more time is required in the following cycles to reach the minimum necessary concentration of the molecular active catalyst in solution to initiate the catalytic process, thus increasing the induction period. Therefore, the shape and surface properties of the obtained catalyst have impact on kinetics of the reaction only at the initial heterogeneous stage, where the rate of palladium leaching defines the duration of the induction period. Increasing surface area to reduce the induction period in repeated reaction cycles would be countered by increased leaching of palladium in the first cycles, as evident from the comparison between the 3d printed and powder catalyst (Table 1).

3. Conclusions

In this work we demonstrated that SLS 3d printing can be used to fabricate durable objects with catalytic activity for Suzuki-Miyaura cross-coupling reaction by using a commercially available catalyst (palladium NPs on silica, SilicaCat Pd^0 R815-100 by SiliCycle) as the catalytically active additive and polypropylene as the supporting polymer. The obtained 3d printed objects retained the activity of the catalyst additive, while greatly improving practical reusability and reducing the amount of leached palladium. The catalyst operates in pseudo-homogeneous mode: after the initial heterogeneous oxidative addition reaction between the supported palladium and aryl iodide, the active catalyst is transferred into solution as molecular species, which then act as homogeneous catalyst. Neither supported nor leached palladium NPs seem to contribute to the catalysis. Such catalytic mode of operation appears to stem from the catalytically active Pd/SiO_2 additive itself. Therefore, SLS 3d printing greatly improves the usability of a solid heterogeneous Pd/SiO_2 pre-catalyst without altering its chemical behaviour.

Based on this and our previously published work,[17,18] we believe that SLS 3d printing may become a valuable and versatile preparation method in the field of heterogeneous catalysis. However, as is apparent from the recent literature, the search for truly heterogeneous catalysts for Suzuki-Miyaura and other cross-coupling reactions remains a demanding and challenging task, and (at least partially) pseudo-homogeneous mode of catalysis by leached palladium is commonly observed for various supported palladium NP catalysts. While purely heterogeneous and leaching-free catalysts for cross-coupling reactions will remain a highly desired goal, the SLS 3d printing offers great advantages already within the realms of pseudo-homogeneous catalysis, such as reduced palladium leaching and improved practical reusability.

Experimental Section

Preparation of the 3d printed catalyst

The materials were used as received from the commercial sources without any pre-treatment. Polypropylene (131.7 g, Adsint PP Flex, BASF) and commercially available palladium NPs on silica (22 g, SilicaCat Pd^0 R815-100 by SiliCycle, uniform NPs in the range of 2–6 nm, palladium load 0.24 mmol/g) were mixed and thoroughly ground to obtain a homogeneous grey powder with calculated 0.034 mmol/g palladium content, which was then used for 3d printing. The sleeves were designed in FreeCAD (v. 0.16), the produced 3d models were converted into G-code (0.1 mm layers) using Slic3r software (v. 1.2.9) and manufactured using an SLS 3d printer Sharebot Snowwhite. The following printing parameters were used: powder temperature 135 °C, laser power 30% (4.2 W), laser speed 1900 mm/s. After printing, the sleeves were cleaned and thoroughly washed with water and ethanol to remove loose

powder, dried in an oven at 110 °C for 48 h, and stored in a desiccator.

Suzuki-Miyaura cross-coupling and leaching tests

The catalytic tests were conducted under argon using standard Schlenk techniques to avoid inconsistencies due to atmospheric variations and possible degradation of reaction intermediates in solution. Unused stirring bars were used to avoid the influence of possible palladium contamination in PTFE coating on the reactions.[30] Methanol (Fischer Scientific, analytical reagent grade) was distilled and stored over activated molecular sieves 3 Å under argon; other chemicals were purchased from Sigma-Aldrich and used as received without further purification.

In a typical Suzuki-Miyaura cross-coupling reaction, phenylboronic acid pinacol ester (1.2 eq.), K_2CO_3 (1.5 eq.), catalyst (approximately 5 μmol or 0.2–0.5 mol% of palladium) as two 3d printed sleeves (130–180 mg) or SilicaCat powder (22–30 mg), and dodecane (1 eq., internal standard) were mixed in methanol (20 or 50 ml depending on the reagent loads to keep a constant 0.05 M concentration of dodecane). The obtained mixture was heated to reflux, and aryl iodide (1 eq.) was added. At this moment, counting of the reaction time began, and the mixture was refluxed with stirring for up to 4 h. The detailed descriptions of representative test reactions are presented in the supporting information.

For recycling after the typical reactions, the catalysts were removed from the reaction mixtures with a magnetic rod (3d printed sleeves, Figure S1) or by filtering off the reaction solution (SilicaCat powder, Figure S2), rinsed with methanol (10 ml) and vacuum-dried prior to re-use. The loss of palladium due to leaching was not accounted in the consequent cycles.

In the filtration tests (section 2.4.1.1), typical reactions with the 3d printed catalyst were performed, and after 10 min of reflux and complete dissolution of the base, the solutions were filtered through 0.45 μm PTFE filters (VWR) into empty flasks with unused magnetic stirring bars. The temperature of the solutions was not maintained during the filtration. The obtained mixtures without the solid catalysts were then refluxed for 3 h.

In the chelation test with poly(4-vinylpyridine) (PVPy, section 2.4.1.2), typical reactions with the 3d printed catalyst were conducted with addition of 174 mg (approximately 300 eq. relative to palladium) of PVPy (2% cross-linked with divinylbenzene, powder, Sigma-Aldrich) before start of the reaction.

In the base-promoted homogeneous catalysis tests (section 2.4.1.3), the 3d printed catalyst (two 3d printed sleeves, 126 mg) was refluxed with stirring in methanol (25 ml) with K_2CO_3 (1.5 mmol) for 3 h. The yellowish solution was filtered without maintaining its temperature through a 0.45 μm PTFE filter (VWR) into a flask containing 4-fluorophenyl iodide (1 mmol), phenylboronic acid pinacol ester (1.2 mmol.), K_2CO_3 (1.5 mmol), dodecane (1 mmol) and an unused magnetic stirring bar, and the obtained mixture without the solid catalyst was refluxed for 4 h.

In the 4-fluorophenyl iodide promoted homogeneous catalysis tests (section 2.4.1.3), the 3d printed catalyst (two 3d printed sleeves, 126 mg) was refluxed with stirring in methanol (25 ml) with K_2CO_3 (1.5 mmol) and 4-fluorophenyl iodide (1 mmol) for 3 h. The greenish solution was filtered without maintaining its temperature through a 0.45 μm PTFE filter (VWR) into a flask containing phenylboronic acid pinacol ester (1.2 mmol.), K_2CO_3 (1.5 mmol), dodecane (1 mmol) and an unused magnetic stirring bar, and the obtained mixture without the solid catalyst was refluxed for 4 h.

In the leaching tests (section 2.4.2), the 3d printed catalysts (one sleeve, 65–100 mg) were refluxed with stirring in methanol (10 ml) with K_2CO_3 (0.75 mmol), 4-fluorophenyl iodide (0.5 mmol, in the 4-fluorophenyl iodide promoted leaching tests) and PVPy (86.6 mg, in the chelating tests with PVPy) for 3 h. The obtained solutions were thoroughly filtered through cotton filters prior to analysis.

Characterization methods

The reaction solutions were analyzed by withdrawing 2 ml aliquots from reaction mixtures at recorded time points. Reaction yields were determined by gas chromatography – mass spectrometry (GCMS). Samples (40 μl) were diluted to 0.2–0.5 mM concentration in HPLC grade methanol (J.T. Baker) and analyzed with a Shimadzu GCMS-QP2010 Plus with Supelco β-DEX 120 column or Agilent 6890 GC with Zebron ZB-5MSi column and 5973 MS detector using helium as carrier gas. The quantities were determined using calibration with dodecane ($C_{12}H_{26}$) as an internal standard.

The palladium content in solution was determined by inductively coupled plasma – optical emission spectrometry (ICP-OES). Samples (1.5 ml) were evaporated to dryness, 1 ml of aqua regia was added, and the samples were digested for 24 h. The samples were then diluted with ultrapure water (18.2 MΩ cm resistivity) and analyzed with PerkinElmer Optima 8300 ICP-OES. The analysis was done using GemCone low flow nebulizer along with cyclonic spray chamber. For the measurements, RF power of 1500 W was used with argon gas flow of 8 l/min, nebulizer flow of 0.7 l/min, auxiliary flow of 0.2 l/min and sample flow rate of 1.5 ml/min. The measurements were performed using an emission wavelength of 340.458 nm. Calibration of the instrument was done using solutions with 0.05, 0.5 and 5 mg/l of palladium and R^2-value of $\geq$ 0.9999 was maintained for the calibration.

Scanning electron microscopy (SEM) was performed using a Zeiss EVO 50 microscope. Samples were prepared by slicing off surface pieces (outer surface samples) of the sleeves or by cutting the sleeves radially and slicing the internal rings (internal structure samples), and coated with gold using sputter deposition.

Acknowledgements

We thank the SA/DAAD (PPP programme, SA Proj. no. 316211, DAAD Proj. ID 57404928) for financial support for mutual exchange visits.

Conflict of Interest

The authors declare no conflict of interest.

Keywords: 3d printing · Suzuki-Miyaura cross-coupling · palladium nanoparticles · selective laser sintering

[1] C. Zhu, Z. Qi, V. A. Beck, M. Luneau, J. Lattimer, W. Chen, M. A. Worsley, J. Ye, E. B. Duoss, C. M. Spadaccini, C. M. Friend, J. Biener, *Sci. Adv.* **2018**, *4*, eaas9459.
[2] A. J. Young, R. Guillet-Nicolas, E. S. Marshall, F. Kleitz, A. J. Goodhand, L. B. L. Glanville, M. R. Reithofer, J. M. Chin, *Chem. Commun.* **2019**, *55*, 2190–2193.
[3] C. A. Leclerc, R. Gudgila, *Ind. Eng. Chem. Res.* **2019**, *58*, 14632–14637.

[4] A. Sanchez Díaz-Marta, S. Yáñez, C. R. Tubío, V. L. Barrio, Y. Piñeiro, R. Pedrido, J. Rivas, M. Amorín, F. Guitián, A. Coelho, *ACS Appl. Mater. Interfaces* **2019**, *11*, 25283–25294.
[5] M. P. Browne, J. Plutnar, A. M. Pourrahimi, Z. Sofer, M. Pumera, *Adv. Energy Mater.* **2019**, *9*, 1900994.
[6] S. Chang, X. Huang, C. Y. A. Ong, L. Zhao, L. Li, X. Wang, J. Ding, *J. Mater. Chem. A* **2019**, *7*, 18338–18347.
[7] C. R. Tubío, J. Azuaje, L. Escalante, A. Coelho, F. Guitián, E. Sotelo, A. Gil, *J. Catal.* **2016**, *334*, 110–115.
[8] A. Quintanilla, J. Carbajo, J. A. Casas, P. Miranzo, M. I. Osendi, M. Belmonte, *Catal. Today* **2019**, In Press, DOI https://doi.org/10.1016/j.cattod.2019.06.026.
[9] V. Middelkoop, A. Vamvakeros, D. de Wit, S. D. M. Jacques, S. Danaci, C. Jacquot, Y. de Vos, D. Matras, S. W. T. Price, A. M. Beale, *J. CO2 Util.* **2019**, *33*, 478–487.
[10] F. Magzoub, X. Li, J. Al-Darwish, F. Rezaei, A. A. Rownaghi, *Appl. Catal. B* **2019**, *245*, 486–495.
[11] A. Sangiorgi, Z. Gonzalez, A. Ferrandez-Montero, J. Yus, A. J. Sanchez-Herencia, C. Galassi, A. Sanson, B. Ferrari, *J. Electrochem. Soc.* **2019**, *166*, H3239–H3248.
[12] V. Middelkoop, T. Slater, M. Florea, F. Neaţu, S. Danaci, V. Onyenkeadi, K. Boonen, B. Saha, I.-A. Baragau, S. Kellici, *J. Cleaner Prod.* **2019**, *214*, 606–614.
[13] J. S. Manzano, H. Wang, I. I. Slowing, *ACS Appl. Polym. Mater.* **2019**, *1*, 2890–2896.
[14] E. Lahtinen, M. M. Hänninen, K. Kinnunen, H. M. Tuononen, A. Väisänen, K. Rissanen, M. Haukka, *Adv. Sustainable Syst.* **2018**, *2*, 1800048.
[15] E. Lahtinen, R. L. M. Precker, M. Lahtinen, E. Hey-Hawkins, M. Haukka, *ChemPlusChem* **2019**, *84*, 222–225.
[16] E. Lahtinen, E. Kukkonen, J. Jokivartio, J. Parkkonen, J. Virkajärvi, L. Kivijärvi, M. Ahlskog, M. Haukka, *ACS Appl. Energy Mater.* **2019**, *2*, 1314–1318.
[17] E. Lahtinen, L. Turunen, M. M. Hänninen, K. Kolari, H. M. Tuononen, M. Haukka, *ACS Omega* **2019**, *4*, 12012–12017.
[18] E. Lahtinen, E. Kukkonen, V. Kinnunen, M. Lahtinen, K. Kinnunen, S. Suvanto, A. Väisänen, M. Haukka, *ACS Omega* **2019**, *4*, 16891–16898.
[19] N. Miyaura, K. Yamada, A. Suzuki, *Tetrahedron Lett.* **1979**, *20*, 3437–3440.
[20] A. Suzuki, *Angew. Chem. Int. Ed.* **2011**, *50*, 6722–6737; *Angew. Chem.* **2011**, *123*, 6854–6869.
[21] C. E. Garrett, K. Prasad, *Adv. Synth. Catal.* **2004**, *346*, 889–900.
[22] M. Mora, C. J.-S. J. R. Ruiz, *Curr. Org. Chem.* **2012**, *16*, 1128–1150.
[23] D. B. Eremin, V. P. Ananikov, *Coord. Chem. Rev.* **2017**, *346*, 2–19.
[24] M. Pérez-Lorenzo, *J. Phys. Chem. Lett.* **2012**, *3*, 167–174.
[25] Y. Zhao, L. Du, H. Li, W. Xie, J. Chen, *J. Phys. Chem. Lett.* **2019**, *10*, 1286–1291.
[26] M. Pagliaro, V. Pandarus, F. Béland, R. Ciriminna, G. Palmisano, P. D. Carà, *Catal. Sci. Technol.* **2011**, *1*, 736–739.
[27] A. Bourouina, V. Meille, C. de Bellefon, *J. Flow Chem.* **2018**, *8*, 117–121.
[28] N. T. S. Phan, M. Van Der Sluys, C. W. Jones, *Adv. Synth. Catal.* **2006**, *348*, 609–679.
[29] M. Pagliaro, V. Pandarus, R. Ciriminna, F. Béland, P. D. Carà, *ChemCatChem* **2012**, *4*, 432–445.
[30] E. O. Pentsak, D. B. Eremin, E. G. Gordeev, V. P. Ananikov, *ACS Catal.* **2019**, *9*, 3070–3081.
[31] G. Han, X. Li, J. Li, X. Wang, Y. S. Zhang, R. Sun, *ACS Omega* **2017**, *2*, 4938–4945.
[32] C. Vollmer, M. Schröder, Y. Thomann, R. Thomann, C. Janiak, *Appl. Catal. A* **2012**, *425–426*, 178–183.
[33] J. A. Gladysz, *Pure Appl. Chem.* **2009**, *73*, 1319–1324.
[34] B. Van Vaerenbergh, J. Lauwaert, J. W. Thybaut, P. Vermeir, J. De Clercq, *Chem. Eng. J.* **2019**, *374*, 576–588.
[35] S. Klingelhöfer, W. Heitz, A. Greiner, S. Oestreich, S. Förster, M. Antonietti, *J. Am. Chem. Soc.* **1997**, *119*, 10116–10120.
[36] W. J. Sommer, K. Yu, J. S. Sears, Y. Ji, X. Zheng, R. J. Davis, C. D. Sherrill, C. W. Jones, M. Weck, *Organometallics* **2005**, *24*, 4351–4361.
[37] K. Yu, W. Sommer, M. Weck, C. W. Jones, *J. Catal.* **2004**, *226*, 101–110.
[38] A. Biffis, P. Centomo, A. Del Zotto, M. Zecca, *Chem. Rev.* **2018**, *118*, 2249–2295.
[39] G. Albano, S. Interlandi, C. Evangelisti, L. A. Aronica, *Catal. Lett.* **2019**, *150*, 652–659.
[40] F. Zhao, B. M. Bhanage, M. Shirai, M. Arai, *Chem. Eur. J.* **2000**, *6*, 843–848.
[41] S. S. Soomro, F. L. Ansari, K. Chatziapostolou, K. Köhler, *J. Catal.* **2010**, *273*, 138–146.
[42] C. Deraedt, D. Astruc, *Acc. Chem. Res.* **2014**, *47*, 494–503.
[43] V. P. Ananikov, I. P. Beletskaya, *Organometallics* **2012**, *31*, 1595–1604.

Manuscript received: May 12, 2020
Revised manuscript received: June 16, 2020
Accepted manuscript online: June 20, 2020
Version of record online: August 11, 2020